Published by IOP Publishing for Sissa Medialab

Received: *October 31, 2023*
Revised: *May 2, 2024*
Accepted: *May 6, 2024*
Published: *May 31, 2024*

24th International Workshop on Radiation Imaging Detectors
Oslo, Norway
25–29 June 2023

Photon Induced Scintillation Amplifier — The PISA concept

C.M.B. Monteiro,* **R.D.P. Mano**, **R.J.C. Roque** and **J.P.G. Neves**

LIBPhys-UC, REAL, University of Coimbra,
3004-516 Coimbra, Portugal

E-mail: cristinam@uc.pt

Abstract: Photoelectron signal amplification in gas photomultipliers (GPMs) is achieved through charge avalanche development in the holes of a cascade of hole-type microperforated foils. When a voltage difference is applied between the metal film electrodes that are deposited on both surfaces of those foils, an electric field with a high intensity is established inside the holes. As a consequence, each electron entering those holes produces an electron avalanche that emerges from the other side of the holes. A cascade of few foils is necessary for a single primary electron to produce a final avalanche intense enough to be read out, in the anode electrode, above the electronic noise. We propose the Photon Induced Scintillation Amplifier (PISA), where the photoelectron signal amplification is obtained by reading out the photon scintillation produced in the charge avalanches of solely one Micro-Hole-and-Strip-Plate-type microstructure with SiPMs. The optical readout has the advantage of having the extra gain from the photosensor and is less sensitive to electronic noise. A large photosensor gain produces large output signals that can travel over long distances without significant degradation. This allows for the readout electronics to be placed away from the photosensor and, thus, from the detector sensitive volume. The scintillation readout plane can be made of a 2D-array of SiPMs, with size and pitch in accordance with the needed scintillation level and position resolution. A first basic prototype was assembled to present a proof-of-principle of the PISA concept.

Keywords: Electron multipliers (gas); Gaseous detectors; Micropattern gaseous detectors (MSGC, GEM, THGEM, RETHGEM, MHSP, MICROPIC, MICROMEGAS, InGrid, etc); Photon detectors for UV, visible and IR photons (gas) (gas-photocathodes, solid-photocathodes)

*Corresponding author.

https://doi.org/10.1088/1748-0221/19/05/C05054

Contents

1 Introduction

The search for rare events, e.g. interactions of hypothetical particles that may compose the elusive dark matter (DM) of the Universe, such as Weakly Interacting Massive Particles (WIMPs) and axion-like particles (APL), and of hypothetical nuclear decays, such as neutrinoless double-beta decay and double electron capture, request for large mass and, thus, large volume detectors. Those phenomena are of faint occurrence probability, and the detection of such events requires a severe suppression of background events resulting from environmental radiation interactions taking place inside the sensitive volume [1–5]. For that purpose, not only those detectors need to be placed underground in a low-background environment but, in addition, a rigorous selection of materials with reduced radioactivity levels is needed.

Xenon and argon are the most promising detection media for the next generation of multi-ton experiments due to their scalability at moderate prices for both direct DM detection [1, 2] and neutrinoless double beta decay [3, 4]. However, the current generation of noble liquid/gas DM detectors is limited by the radioactivity from the detector materials, particularly the photomultiplier tubes (PMTs) used for the detection of primary and secondary scintillation emitted by noble gases. In addition, PMTs also have limitations such as low total area coverage and high cost per unit of area. Large-area hybrid vacuum PMTs as alternatives to standard PMTs are being considered, but this technology still faces problems related with vacuum sealing and high voltage biasing. Furthermore, the large dimensions required for competitiveness limit the spatial resolution that can be achieved. Large area avalanche photodiodes (LAAPDs) [6] have small gain (few hundreds, to be compared to the 10^6 of PMTs), small area (few cm^2, to be compared to the few tens of cm^2 of PMTs), insensitivity to low scintillation levels and high cost per unit of area, limiting their applications as alternatives to PMTs. Although having gains around 10^6, SiPMs have too small active areas to be an alternative by themselves.

Gas Photomultipliers (GPMs) may offer a high-performance alternative at low cost and can be made in large sizes [7–10]. Unlike standard PMTs, GPMs operate with a filling gas. The photoelectrons emitted from the photocathode are driven through a cascade of hole-type microstructure elements where electrons undergo avalanche multiplication in the gas, under the intense electric fields set inside the holes. Usually, the photocathode is deposited on the top surface of the first microstructure of the cascade, facing the GPM window. The anode electrode can be pixelated to allow sub-millimetre position resolution. However, photoelectron signal amplification by means of charge avalanches in the gas medium needs the use of a cascade of multi-elements and the application of voltages of a few kV to produce the necessary charge-signal gain. In addition, the presence of discharges can

2024 JINST 19 C05054

be a limitation. The need for the readout electronics to be close to the anode is also a significant restraint, especially in applications requiring low radioactive background, as is the case in rare event searches. Along the latter issue, the use of THGEMs will be prohibitive due to the high radioactive background of the FR-4 they are made from.

In this work, we propose a simple concept of a new photosensor called the Photon Induced Scintillation Amplifier (PISA), which aims to address the above limitations of GPMs. In section 2 we describe the concept. In section 3 we describe a first basic prototype built as a proof-of-concept, aiming to have an overview/apprehend on the suitability of the amount of scintillation produced in PISA and the imaging capabilities of PISA, when using a commercial array of SiPM as the photosensor. In section 4 we present preliminary results for the images obtained with this prototype.

2 The PISA concept

In PISA, as in standard GPMs, photons impinging the photocathode that is deposited on the surface of a hole-type microstructure element give rise to the emission of photoelectrons that are driven into the holes where an intense electric field causes electron avalanche. The avalanche electrons are collected in the anode electrode on the other surface of the microstructure. However, in PISA, the photoelectron signal is not amplified by reading out the charge avalanche electrons at the anode, but rather by reading out the secondary scintillation produced in those charge avalanches. For that purpose, a suitable photosensor is used and, at present, SiPMs are the best choice due to their high gain, $\sim 10^6$, low voltage biasing and reduced intrinsic radioactivity when compared to PMTs [11, 12].

The PISA concept presents advantages over PMTs, including higher radiopurity, as the materials used for both microstructure and photosensor, e.g. Kapton and silicon, respectively, can be obtained with reduced radioactivity levels. Pisa also presents other significant advantages over standard GPMs, e.g. allowing for the deployment of remote "hot" (radioactive) electronics, since the high gains achieved with the SiPMs enable signal transmission over large distances without significant signal degradation [13, 14]. This enables higher signal-to-noise ratio due to the additional high-gain of the photosensor, being also less prone to electronic noise and radiofrequency pickup. Moreover, the PISA is cost-effective when compared to vacuum PMTs, allows for area coverage above 80% maximizing photon detection efficiency, and can be implemented with large areas. If needed, it can have submillimetre position resolution. PISA is also an alternative for scintillation readout based only on SiPMs, because the SiPM area coverage can be as low as 10%, e.g. by using 1×1 mm^2 SiPMs with 1-cm pitch [14]. When using a readout of only SiPMs an area coverage over 80% is necessary. Hence if the PISA is used instead, a much smaller number of SiPMs is needed. Therefore, PISA is an imaging device with a position resolution that depends on the SiPM dimensions and pitch.

For the filling gas, one having large scintillation yield is required, e.g. xenon and argon [15, 16]. On the one hand, we have shown that a large number of photons are produced in GEM and THGEM electron avalanches operating in xenon and argon, enabling the use of a single microstructure [17]; one electron may produce about 10^5 and 10^4 photons in the charge avalanches of xenon and argon, respectively [17]. However, on the other hand, noble gas emission is in the deep VUV region, where SiPMs are insensitive or have low sensitivity. Therefore, a gas scintillating in the visible range is needed. For that, CF_4 has proven to be a good choice as it is known to present high scintillation output [18, 19]. In addition, noble gas mixtures of lighter noble gases such as Ne or He with CF_4 allow high scintillation output

2024 JINST 19 C05054

with lower applied biasing voltages when compared to pure CF_4 and to Ar-CF_4 mixtures. Both He and Ne could be an alternative to be used in PISA, but Ne has the advantage over He of having much lower diffusion through the quartz GPM window, advantage that could be important for PISA operation, depending on its potential application.

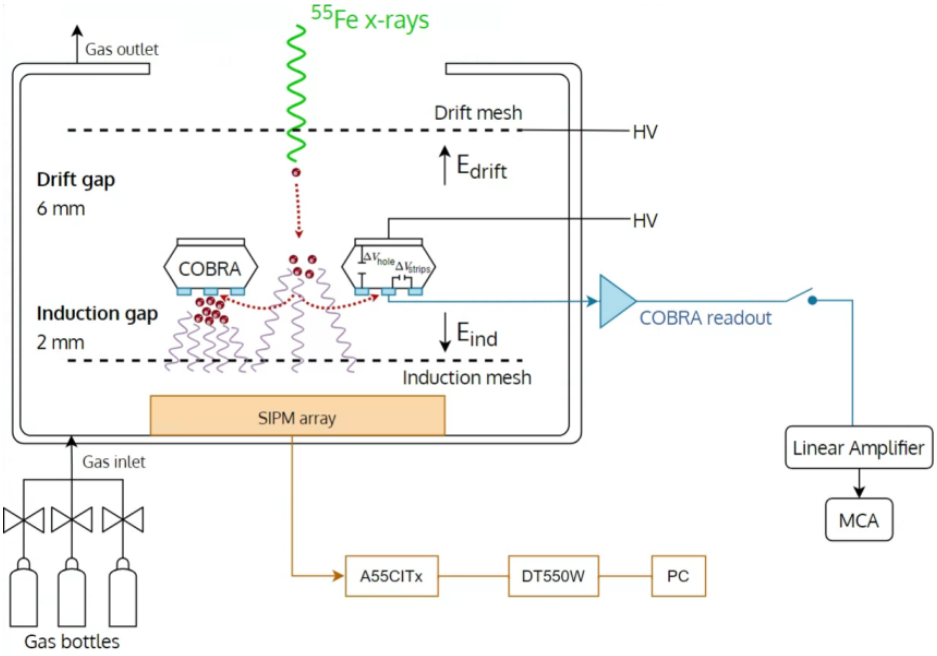

Figure 1. Schematic of the PISA prototype used in this work.

A Micro-Hole-and-Strip-Plate (MHSP) [20, 21], etched on Kapton for radiopurity, can be used instead of the traditional GEM and/or THGEM, since it presents higher photon output due to a second charge avalanche stage, after electrons exiting the holes, around the anode strips etched on the bottom surface of the microstructure foil, figure 1. In addition, the use of a microstructure etched in Kapton foils of 125-µm in thickness [22] allows for higher avalanche gains and robust operation when compared to the standard 50-µm thickness.

3 Experimental setup

A schematic of the PISA prototype used in this work is presented in figure 1. An aluminium chamber of $23 \times 23 \times 5\,\mathrm{cm}^3$ was used to accommodate a drift mesh, an MHSP-foil, an induction mesh, and a photosensor. The charge amplification element is a MHSP-type, the 125-µm thick Cobra [22]: a 125-µm thick Kapton foil coated on both sides with a 5-µm thick Cu film and perforated by biconical holes in a hexagonal pattern. While the upper surface is not structured, on the bottom surface two different strips are etched: the strips surrounding the holes and, between those, the anode strips, figure 2. The meshes are made of stainless-steel wires, 80-µm in diameter, with 900-µm spacing, having 84% optical transmission. The drift region, delimited by the drift mesh and the Cobra, is 6-mm deep and the induction region, between the induction mesh and the Cobra foil is 2-mm thick. Throughout the studies the induction mesh and the anode strips were kept at −130 V and −10 V, respectively. The voltages between the bottom strips surrounding the holes, the top electrode and the

drift mesh were set with increasing negative voltages, while keeping constant the voltage difference across the holes and in the drift region, at 720 V and 250 V, respectively.

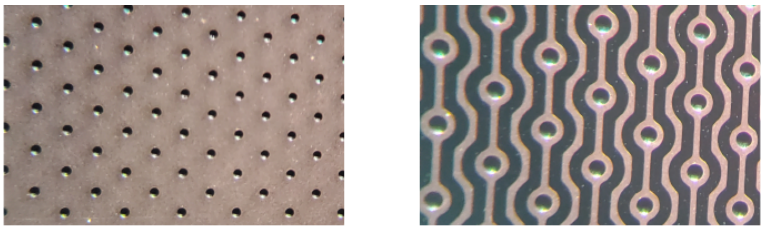

(a) Top electrode (b) Bottom electrode

Figure 2. Photographs of the Cobra-125 µm foil: a) top electrode; b) bottom electrodes.

The photosensor used for the scintillation readout is a Hamamatsu S13361-3050 SiPM unit, which consists of an 8×8 array of 3×3 mm^2 SiPMs with a spectral sensitivity in the 320–900 nm range. Each SiPM includes 3584 Geiger-Avalanche Photodiodes (G-APD) with 50×50 μm^2 area.

For the first studies of the proof-of-concept, we used x-rays from a ^{55}Fe radioactive source, ~2-mm collimated, to produce free electrons in the drift region above the MHSP, instead of a light source irradiating a CsI photocathode producing photoelectrons ejected from the CsI into the drift region. A fraction of the x-rays emitted by the source is absorbed in the gas in the drift region, resulting in ~170 free electrons by photoelectric effect, since the gas w-value is ~34 eV [23]. These free electrons will produce large scintillation pulses, well above the background noise resulting from dark current, and x-ray direct interaction in the SiPMs. The free electrons are driven towards the Cobra holes, under the influence of a weak electric field, where they undergo charge avalanche multiplication in the strong electric field inside those holes. After exiting the holes, the avalanche electrons are guided towards the anode strips, originating a second charge avalanche in the high electric field region around those strips. Along both avalanches a large number of photons are emitted, which are read out by the SiPMs.

Two 50-cm long flexible cables of copper lines in Kapton connect the 24×32 channel output of the SiPM array to a CAEN DT555OW and a A55CITx piggyback data acquisition board, for reading out the signal amplitude of each of the 64 SiPMs individually. Therefore, a 2D image can be acquired resulting from the individual amplitude registered in each SiPM. Upon this, an overall amplitude resulting from the sum of all 64 individual amplitudes can be registered.

The detector was operated in flow mode with a gas flow around 1 dm^3/hour. The uncertainty in the concentrations is less than 0.025% and 0.25%, in absolute value, for CF_4 and He, respectively. He was used instead of Ne for its availability.

4 Experimental results and discussion

With an LED we illuminated each individual SiPM, using 1-mm collimation. We found that both the distribution of the amplitude of each individual SiPM and the distribution of the amplitudes of several measurements in a single SiPM have a standard deviation of 0.2%. Detector background acquisitions were obtained without and with the presence of the ^{55}Fe x-ray source irradiation and without high voltages applied to the microstructure, i.e. without gas scintillation. We used the board facility to remove all the events producing a charge pulse below a given threshold, which we chose to be well above that background. Detector background acquisitions with the high voltages on and without x-ray

2024 JINST 19 C05054

irradiation were obtained. This background is due to eventual tiny micro discharges that result from potential imperfections in the copper electrodes deposited on the Kapton foil surfaces. A 2D-map of the average background was then used to be subtracted from all the raw images.

In addition, an acquisition with the whole area uniformly irradiated by x-rays under gas scintillation conditions was performed to obtain the correction parameter for each SiPM to compensate for detector response nonuniformities, e.g. nonuniformities in the microstructure resulting in different signal amplification in the holes and/or around the anode strips. This 2D-distribution is used to correct the distributions obtained for all the raw images.

In figure 3 we depict the 2D maps of the amplitude distribution, after background subtraction and nonuniformity's correction, for different voltages applied between the Cobra strips and for a constant voltage difference of 720 V across the holes. For low voltage differences, the electric field intensity around the anode strips is not enough to promote electron avalanche and the scintillation read out by the SiPM unit is the scintillation produced in the holes. As the voltage difference between the strips increases, the charge avalanche around the anode strips and, thus, the scintillation produced around the anode strips increases exponentially, resulting in an exponential increase of the scintillation, well above one order of magnitude, figure 4. For the last two highest voltages, it seems that the SiPM enters a non-linear, saturation regimen due to the large scintillation output, which results in a non-negligible probability of more than one photon hitting a single G-APD microcell. Under these conditions the number of photons detected by the SiPM deviates from the exponential growth of the photons produced in the avalanche, figure 4.

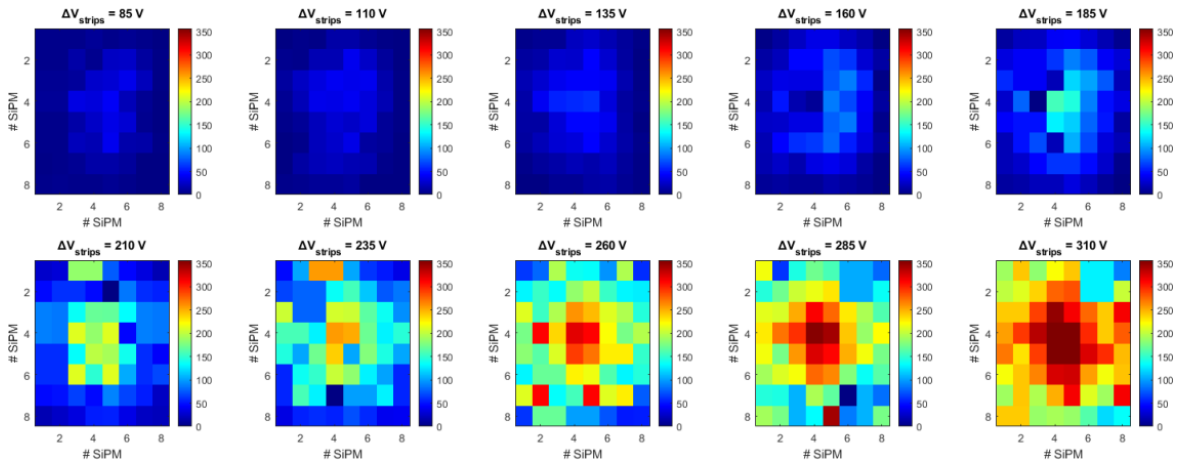

Figure 3. 2D maps of the amplitude distribution in the SiPM array, after background subtraction and nonuniformity's correction, for different voltages between the Cobra strips and for a constant $\Delta V_{\text{hole}} = 720$ V.

As an example of imaging potential of this PISA prototype, figure 5 (left panel) presents the data, after background subtraction and nonuniformity corrections, obtained using 720 V and 260 V potential differences across the holes and between the strips, respectively. Figure 5 further presents an example of subsequent imaging processing to improve image quality, namely the possibility to visualize the image in cell units with subpixel dimensions, by using the interpolation method [24, 25], and then by further applying a Gaussian filter [24] to smooth image intensity variations, ($\sigma = 1$) and ($\sigma = 2$), available in the Matlab libraries.

Figure 6 presents the same features as figure 5, but for a 2-mm wide slit collimator.

2024 JINST 19 C05054

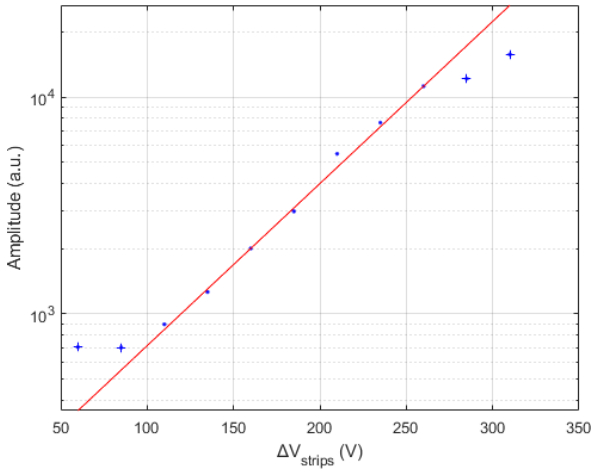

Figure 4. Total amplitude read out from the SiPM array as a function of voltage difference between the bottom strips of the Cobra microstructure.

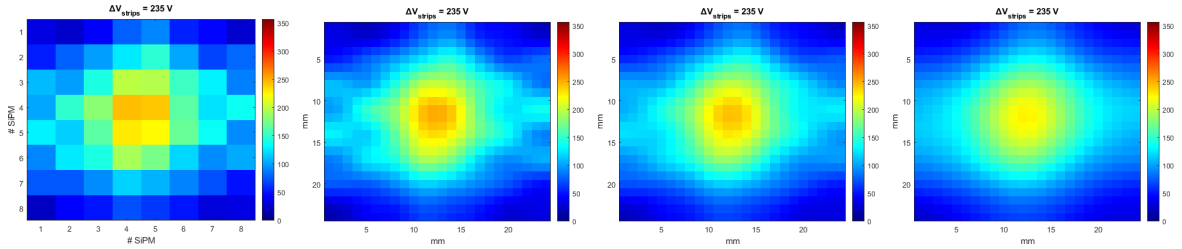

Figure 5. Example of subsequent imaging processing for a 2-mm diameter hole collimator, namely interpolation method and gaussian filter with $\sigma = 1$ and $\sigma = 2$.

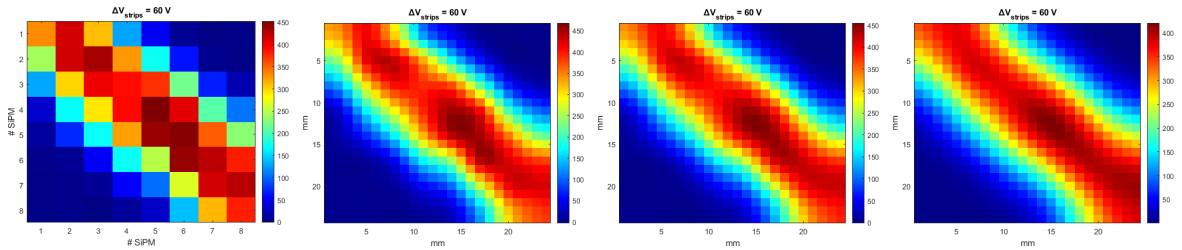

Figure 6. Example of subsequent imaging processing for a 2-mm wide slit collimator, namely interpolation method and gaussian filter with $\sigma = 1$ and $\sigma = 2$.

5 Conclusions

We have presented the PISA concept as an alternative to gaseous photomultipliers. Instead of using the standard charge readout for the photoelectron signal amplification, PISA uses a suitable photosensor to read out the scintillation produced in the charge avalanches. A basic prototype was implemented as proof-of-concept, using an 8×8, 3 mm^2, SiPM array. The imaging potential of this prototype was demonstrated.

Future work will focus on the measurement of the absolute scintillation yield of He-CF_4 and Ne-CF_4 mixtures to demonstrate the PISA capability for single photon readout. The number of

2024 JINST 19 C05054

photons released in avalanches that are produced by one single electron should be large enough in order to yield a signal output above the background in the SiPM readout unit, taking into account the quantum efficiency of the SiPMs and the effective area covered by them.

Acknowledgments

This work is supported by DOI:10.54499/CEECIND/04434/2017/CP1460/CT0027, CERN/FIS-TEC/0038/2021, CERN/FIS-INS/0026/2019, UIDB/FIS/04559/2020 and UIDP/FIS/04559/2020 (LIBPhys), funded by national funds through FCT/MCTES and co-financed by the European Regional Development Fund (ERDF) through the Portuguese Operational Program for Competitiveness and Internationalization, COMPETE 2020.

References

[1] DARWIN collaboration, M. Adrover et al., *Cosmogenic background simulations for neutrinoless double beta decay with the DARWIN observatory at various underground sites*, *Eur. Phys. J. C* **84** (2024) 88 [arXiv:2306.16340].

[2] T.N. Thorpe, *The DarkSide-20k TPC and underground argon cryogenic system*, *SciPost Phys. Proc.* **12** (2023) 069 [arXiv:2210.00322].

[3] NEXT collaboration, C. Adams et al., *Sensitivity of a tonne-scale NEXT detector for neutrinoless double beta decay searches*, *JHEP* **08** (2021) 164 [arXiv:2005.06467].

[4] S. Obara et al., *AXEL: High-pressure Xe gas TPC for BG-free* $0\nu2\beta$ *decay search*, *Nucl. Instrum. Meth. A* **958** (2020) 162803 [arXiv:1909.09343].

[5] NEXT collaboration, C.A.O. Henriques et al., *Neutral Bremsstrahlung Emission in Xenon Unveiled*, *Phys. Rev. X* **12** (2022) 021005 [arXiv:2202.02614].

[6] L.M.P. Fernandes et al., *Characterization of large area avalanche photodiodes in X-ray and VUV-light detection*, 2007 *JINST* **2** P08005 [physics/0702130].

[7] C.D.R. Azevedo et al., *Towards THGEM UV-photon detectors for RICH: On single-photon detection efficiency in Ne/CH(4) and Ne/CF(4)*, 2010 *JINST* **5** P01002 [arXiv:0909.5357].

[8] A. Breskin et al., *CsI-THGEM gaseous photomultipliers for RICH and noble-liquid detectors*, *Nucl. Instrum. Meth. A* **639** (2011) 117 [arXiv:1009.5883].

[9] S. Duval et al., *Hybrid Multi Micropattern Gaseous Photomultiplier for detection of liquid-xenon scintillation*, *Nucl. Instrum. Meth. A* **695** (2012) 163 [arXiv:1110.6053].

[10] L. Arazi et al., *First results of a large-area cryogenic gaseous photomultiplier coupled to a dual-phase liquid xenon TPC*, 2015 *JINST* **10** P10020 [arXiv:1508.00410].

[11] NEXT collaboration, S. Cebrián et al., *Radiopurity assessment of the tracking readout for the NEXT double beta decay experiment*, 2015 *JINST* **10** P05006 [arXiv:1411.1433].

[12] V. Álvarez et al., *Radiopurity control in the NEXT-100 double beta decay experiment: procedures and initial measurements*, 2013 *JINST* **8** T01002 [arXiv:1211.3961].

[13] NEXT collaboration, V. Alvarez et al., *Operation and first results of the NEXT-DEMO prototype using a silicon photomultiplier tracking array*, 2013 *JINST* **8** P09011 [arXiv:1306.0471].

[14] NEXT collaboration, F. Monrabal et al., *Initial results on energy resolution of the NEXT-White detector*, 2018 *JINST* **13** P10020 [arXiv:1808.01804].

2024 JINST 19 C05054

[15] C.M.B. Monteiro et al., *Secondary Scintillation Yield in Pure Xenon*, 2007 *JINST* **2** P05001 [physics/0702142].

[16] C.M.B. Monteiro, J.A.M. Lopes, J.F.C.A. Veloso and J.M.F. dos Santos, *Secondary scintillation yield in pure argon*, *Phys. Lett. B* **668** (2008) 167.

[17] C.M.B. Monteiro et al., *Secondary scintillation yield from GEM and THGEM gaseous electron multipliers for direct dark matter search*, *Phys. Lett. B* **714** (2012) 18.

[18] M.M.F.R. Fraga et al., *The GEM scintillation in He CF-4, Ar CF-4, Ar TEA and Xe TEA mixtures*, *Nucl. Instrum. Meth. A* **504** (2003) 88.

[19] F.D. Amaro et al., *The CYGNO experiment, a directional detector for direct Dark Matter searches*, *Nucl. Instrum. Meth. A* **1054** (2023) 168325 [arXiv:2306.04568].

[20] J.F.C.A. Veloso, J.M.F. dos Santos and C.A.N. Conde, *A proposed new microstructure for gas radiation detectors: The microhole and strip plate*, *Rev. Sci. Instrum.* **71** (2000) 2371.

[21] J.M. Maia et al., *Advances in the Micro-Hole & Strip Plate gaseous detector*, *Nucl. Instrum. Meth. A* **504** (2003) 364.

[22] F.D. Amaro et al., *Operation of a novel large area, high gain, single stage gaseous electron multiplier*, 2021 *JINST* **16** P01033.

[23] G.F. Reinking, L.G. Christophorou and S.R. Hunter, *Studies of total ionization in gases/mixtures of interest to pulsed power applications*, *J. Appl. Phys.* **60** (1986) 499.

[24] R.C. Gonzalez and R.E. Woods, *Digital Image Processing*, Fourth Edition, Pearson Education © (2018) [ISBN: 978-0-13-335672-4].

[25] http://www.mathworks.com/.

2024 JINST 19 C05054